IOPscience iopscience.iop.org

Home Search Collections Journals About Contact us My IOPscience

Nature of Friedel oscillations around Si dopants in the GaAs(110) accumulation layer

This article has been downloaded from IOPscience. Please scroll down to see the full text article.

2000 J. Phys.: Condens. Matter 12 L489

(http://iopscience.iop.org/0953-8984/12/30/102)

View the table of contents for this issue, or go to the journal homepage for more

Download details:
IP Address: 171.66.16.221
The article was downloaded on 16/05/2010 at 05:25

Please note that terms and conditions apply.

J. Phys.: Condens. Matter **12** (2000) L489–L496. Printed in the UK PII: S0953-8984(00)14848-9

LETTER TO THE EDITOR

Nature of Friedel oscillations around Si dopants in the GaAs(110) accumulation layer

J E Inglesfield†, M H Boon‡ and S Crampin§

† Department of Physics and Astronomy, University of Wales Cardiff, PO Box 913, Cardiff, CF2 3YB, UK

‡ Institute for Theoretical Physics, University of Nijmegen, PO Box 9010, NL-6500 GL Nijmegen, Netherlands

§ Department of Physics, University of Bath, Bath, BA2 7AY, UK

Received 20 June 2000

Abstract. The screening of sub-surface Si impurities in an accumulation layer at the GaAs(110) surface is calculated. Such an accumulation layer can be induced by a scanning tunnelling microscope tip, and surface Friedel oscillations have been imaged around the Si dopants. This study uses the effective mass approximation to describe the electrons in the GaAs conduction band, and a fitted model potential for the impurity. Two-dimensional effects dominate, with a doubly occupied bound state pulled off the lowest sub-band by the impurity, and a depletion of one electron in the conduction states. The bound state gives a large central peak in the surface induced charge, with the Friedel oscillations coming from the change in the conduction states. To explain the amplitude of the observed oscillations, it is necessary to reduce the tunnelling contribution from the bound state.

In low-temperature scanning tunnelling microscopy (STM) experiments on n-type GaAs(110), biased to induce an accumulation layer at the surface, surface Friedel oscillations have been measured around sub-surface Si donor impurities [1, 2]. These show up in constant-current measurements as an oscillatory height variation around a central peak. It was thought that room temperature measurements show only the hillock above the dopants [3], though it is now apparent that a very weak oscillation can be seen under these conditions around Si impurities in the surface layer [4], and even around sub-surface Si [5]. Previous theory has studied STM imaging of Friedel oscillations around an impurity in a semi-infinite electron gas [6]. In other work, the screened potential around a surface impurity has been fitted to experiment, and this was then used to estimate the change in surface density of states and tunnelling current [4]. Friedel oscillations have also been studied, using scanning tunnelling spectroscopy, around sub-surface donor impurities at InAs(110), and the results fitted by a WKB treatment of the screening electrons [7].

In this Letter we shall calculate the screening around an impurity by the electrons confined by the accumulation layer potential, and we shall show the importance of the reduced dimensionality. We use a model impurity potential, as our aim is to study general features associated with impurities in an accumulation layer. We find that the screening charge has two contributions—a doubly-occupied (D^-) impurity bound state which dominates the central peak in the image, and a loss of one electron through the occupied conduction band associated with the first minimum and successive Friedel oscillations. Finally we shall relate this to the STM measurements.

The experiments which we shall consider were performed on Si-doped GaAs, with an impurity density of 2×10^{18} cm^{-3} [1]. The Si substitutes for Ga, and acts as a donor with an

0953-8984/00/300489+08$30.00 © 2000 IOP Publishing Ltd

ionization energy of 2 meV. In a typical configuration the STM tip was separated by 10 Å from the GaAs(110) surface, and using a sample bias of −2.5 V there is an electron accumulation layer with an estimated surface band bending of 0.28 eV. Thus the Fermi energy is 0.28 eV above the bottom of the conduction band at the surface. In STM measurements at 4.2 K the Si impurities image as a central peak, with an apparent height of typically 1 Å, beyond which there are Friedel oscillations with the wavelength expected for an electron gas with effective mass $m^* = 0.067m_e$ (appropriate to GaAs), and the local Fermi energy. The impurities can be imaged from many layers below the surface. From the number of observed impurities it is estimated that the maximum depth imaged is about 30 Å [8], or even as deep as 60 Å in some experiments [7].

To calculate the electron states with an impurity in the accumulation layer we use the effective mass approximation, modelling the Si impurity by a parametrized potential which we adjust so that there is one extra electron in the system. First we calculate the band-bending self-consistently, solving the effective mass Schrödinger equation with the Hartree potential due to the filled conduction states. We neglect exchange-correlation, on the grounds that the electron density parameter r_s in the accumulation layer is relatively small, $0.27a^*$ in terms of the effective Bohr radius a^* [9]. The electron states in this potential $V(z)$ (z is the coordinate perpendicular to the surface) are found using a Green function method, with the boundary condition that the amplitude vanishes at the surface. (In previous work we have found that the resulting envelope function gives a good description of the actual wave-functions at the GaAs(110) surface [10].) The Fermi energy and energy zero are at the conduction band minimum at $z = \infty$.

The result of this calculation is that with a sample bias voltage of −2.5 V and a tip-surface distance of 10 Å the surface band-bending is 0.35 eV, somewhat greater than the value of 0.28 eV from a semi-classical calculation [11]. The reason for this difference is that the boundary condition on the wave-functions and their quantization reduce the density near the surface, so greater band-bending is needed to give the total surface charge density required by Gauss's theorem. Figure 1 shows the local density of states at $z = 10$ Å with the quantized sub-bands characteristic of quantum confinement. This quantization has been detected

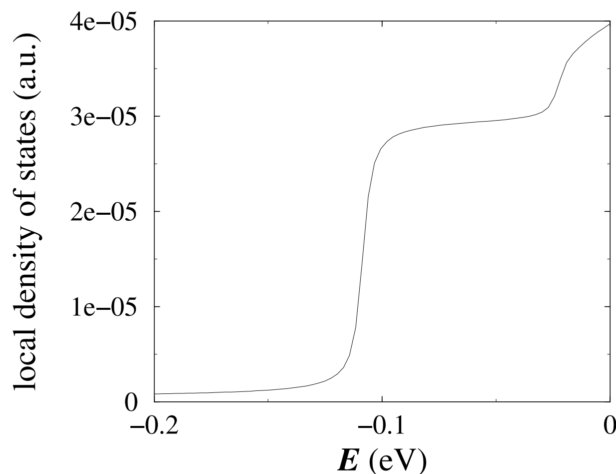

Figure 1. Local density of states (in Hartree atomic units) at $z = 10$ Å. The energy has an imaginary part of 2.7 meV.

in scanning tunnelling spectroscopy [2, 12]. The bottom of the conduction band is at -0.11 eV, much higher than the local potential near the surface.

The electronic structure of the screened impurity can be found using the matching Green function method [13]. The Green function for the whole system is built up from the Green function G_0 for the unperturbed accumulation layer, and the Green function G_{imp} for the impurity by itself. This method relies on being able to separate the system into two parts—an unperturbed region (A) beyond the impurity, and the impurity region (B). To this end we assume that the potential $v(\boldsymbol{r})$ felt by an electron has Coulomb form inside a sphere of radius ρ centred on the impurity at $\boldsymbol{r}_0$, and outside it is given by the accumulation layer potential $V(z)$

$$\begin{aligned} v(\boldsymbol{r}) &= \frac{Z_{\mathrm{eff}} e^2}{|\boldsymbol{r}-\boldsymbol{r}_0|} + V(z_0) \qquad |\boldsymbol{r}-\boldsymbol{r}_0| < \rho \\ &= V(z) \qquad |\boldsymbol{r}-\boldsymbol{r}_0| > \rho. \end{aligned} \tag{1}$$

We treat Z_{eff} and ρ as parameters, though in principle Z_{eff} is given by $-1/\epsilon$.

In the matching Green function formalism, the Green function for the combined system of A joined on to B is given by

$$\begin{aligned} G(\boldsymbol{r},\boldsymbol{r}') = G_0(\boldsymbol{r},\boldsymbol{r}') - \frac{\hbar^2}{2m^*}\int_S \mathrm{d}\boldsymbol{r}_S \left[G_0(\boldsymbol{r},\boldsymbol{r}_S)\frac{\partial G}{\partial n_S}(\boldsymbol{r}_S,\boldsymbol{r}') \right. \\ \left. - \frac{\partial G_0}{\partial n_S}(\boldsymbol{r},\boldsymbol{r}_S) G(\boldsymbol{r}_S,\boldsymbol{r}') \right] \qquad \boldsymbol{r},\ \boldsymbol{r}' \text{ in } A \end{aligned} \tag{2}$$

$$\begin{aligned} G(\boldsymbol{r},\boldsymbol{r}') = \frac{\hbar^2}{2m^*}\int_S \mathrm{d}\boldsymbol{r}_S \left[G_{\mathrm{imp}}(\boldsymbol{r},\boldsymbol{r}_S)\frac{\partial G}{\partial n_S}(\boldsymbol{r}_S,\boldsymbol{r}') - \frac{\partial G_{\mathrm{imp}}}{\partial n_S}(\boldsymbol{r},\boldsymbol{r}_S) G(\boldsymbol{r}_S,\boldsymbol{r}') \right] \\ \boldsymbol{r} \text{ in} B,\ \boldsymbol{r}' \text{ in } A \end{aligned} \tag{3}$$

where n_S is the outward normal derivative from B to A across S, the surface separating A and B. So knowing the surface values of G and $\partial G/\partial n_S$ for fixed $\boldsymbol{r}'$, we can find the Green function for $\boldsymbol{r}$ in both A and B. By putting $\boldsymbol{r}$ on the boundary in both equations we obtain two simultaneous integral equations for the two surface functions. In a spherical harmonic expansion over S in which $G_0(\boldsymbol{r}_S,\boldsymbol{r}'_S)$ becomes matrix $\mathcal{G}_0$ and $G_0(\boldsymbol{r}_S,\boldsymbol{r}')$ vector g_0, and taking G_{imp} to satisfy a zero-derivative boundary condition at ρ, these are given by

$$g' = \left[\left(1 - \frac{\hbar^2}{2m^*}\mathcal{G}'_0\right)\frac{\hbar^2}{2m^*}\mathcal{G}_{\mathrm{imp}} + \frac{\hbar^2}{2m^*}\mathcal{G}_0 \right]^{-1} g_0 \qquad g = \frac{\hbar^2}{2m^*}\mathcal{G}_{\mathrm{imp}} g'. \tag{4}$$

Substituting back into (2) and (3), and using similar expressions for $\boldsymbol{r}'$ in B, gives us the Green function everywhere. The numerical evaluation of $\mathcal{G}_0$ and $\mathcal{G}'_0$ is somewhat tricky, because of the singularity in the Green function. However we can include this by adding and subtracting the free-electron Green function, as we shall describe in a subsequent paper.

The integrated density of states in the combined system, the number of states in the system with energy less than E, can be found from the surface Green functions in (4). The change in the integrated density of states due to the impurity, including spin degeneracy, is given by

$$\delta N(E) = -\frac{2}{\pi}\Im\mathrm{m}\ln\det\left[\left(1 - \frac{\hbar^2}{2m^*}\mathcal{G}'_0\right)\frac{\hbar^2}{2m^*}\mathcal{G}_{\mathrm{imp}} + \frac{\hbar^2}{2m^*}\mathcal{G}_0 \right] + N_{\mathrm{imp}}(E) \tag{5}$$

where N_{imp} is the integrated density of states of the isolated impurity [14]. The energy in (5) is evaluated with a small positive imaginary part. This expression, a generalization of Levinson's theorem [15], enables us to adjust the impurity potential to achieve the self-consistent requirement that there is one extra electron below the Fermi energy, with $\delta N(E_{\mathrm{F}}) = 1$.

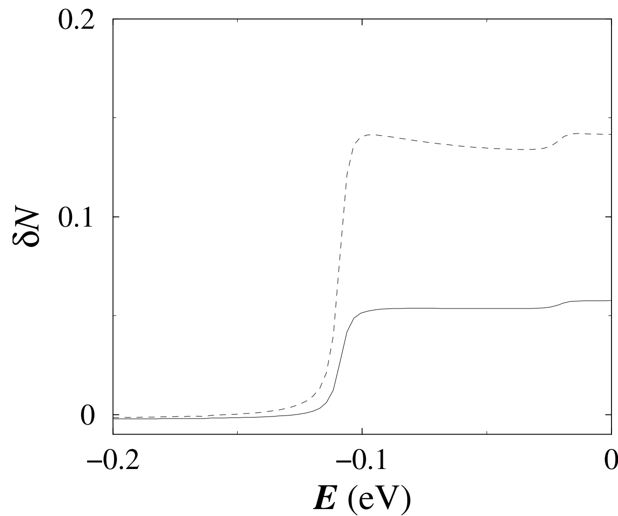

Figure 2. Change in the integrated density of states due to impurity potentials with $Z_{\rm eff} = -0.1$ (solid line) and $Z_{\rm eff} = -0.2$ (dashed line), $\rho = 10$ Å, at $z_0 = 40$ Å. The energy has an imaginary part of 2.7 meV.

The effect of a weak impurity potential on the integrated density of states in the accumulation layer is shown in figure 2. Results are given for an impurity at $z_0 = 40$ Å with the relatively small radius of $\rho = 10$ Å—the number of induced electrons up to $E_{\rm F}$ is only 0.06 with $Z_{\rm eff} = -0.1$. δN shows steps, broadened by the imaginary energy of 2.7 meV, at the threshold energies of the sub-bands (figure 1); the steps in δN correspond to sharp peaks in the actual density of states. Now an attractive potential always pulls off a bound state in two dimensions, though the binding energy may be very small (it varies with the strength of the potential v as $\exp(-\alpha/v)$ [16]). This means that a step in δN which is less than two must be a combination of a bound state just below the sub-band threshold together with a reduction in the number of continuum states directly above.

The energy distribution of states changes greatly when the potential is strong enough to induce one extra electron in the system. Figure 3 shows δN for two impurity potentials inside the semiconductor which satisfy this requirement ($Z_{\rm eff} = -0.26$, $\rho = 25$ Å, at $z_0 = 30$ Å, and $Z_{\rm eff} = -0.15$, $\rho = 40$ Å, at $z_0 = 40$ Å). The bound state is now apparent as a step approaching two in δN—rounded off, and reduced in height, by the imaginary part of the energy which broadens the state. There is a large reduction in the number of states in the continuum above the bottom of the first sub-band, and it is the combination of the bound state with this depletion which leads to $\delta N(E_{\rm F}) = 1$. The loss of continuum states above a nearby bound state is well known from the behaviour of phase shifts in potential scattering. Filling up the states, we have a doubly occupied D^- impurity level, and a net loss of one electron in the occupied continuum states.

There is much evidence from magneto-optic studies for the formation of stable D^- centres on Si donors in GaAs/GaAlAs quantum well structures [17–20]. The binding energy is greatly enhanced in the quasi-two dimensional systems compared with the bulk [21], where D^- centres are only populated under certain sample and experimental conditions [22]. The total energy of the D^- state in a quantum well 100 Å wide has been calculated to be -14 meV, taking the bottom of the lowest sub-band as the energy zero [23]; in our case the loss of one electron

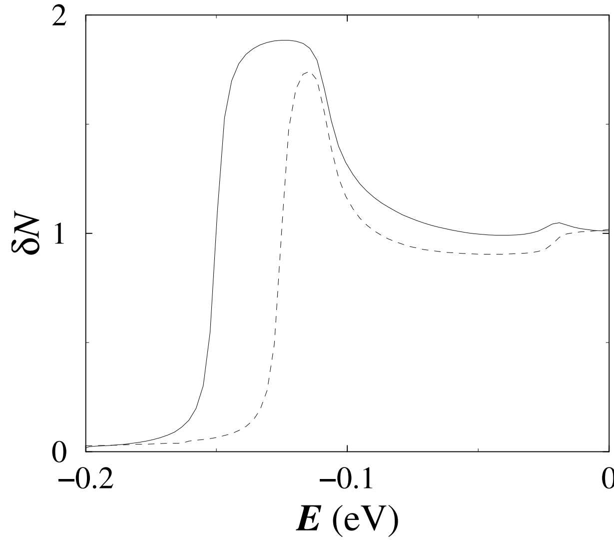

Figure 3. Change in the integrated density of states due to impurity potentials with $Z_{\mathrm{eff}} = -0.26$, $\rho = 25$ Å, at $z_0 = 30$ Å (solid line); and $Z_{\mathrm{eff}} = -0.15$, $\rho = 40$ Å, at $z_0 = 40$ Å. The energy has an imaginary part of 2.7 meV. Both of these impurity potentials add one extra electron to the system.

in the continuum will presumably reduce the electron–electron interaction and increase the binding energy.

As the occupied conduction electron states, including the bound state, come from a very narrow energy range, the tunnelling through the surface potential barrier in the STM experiments is quite constant [10]. So we expect that it is the electron density at the surface which is probed, rather than the local density of states at E_{F}, as was assumed by Kobayashi [6]. In our calculation the wave-functions go to zero at $z = 0$, so we take the tunnelling current in STM to be proportional to the electron density just inside the surface, at $z = 5$ Å (the precise distance does not change the conclusions). Figure 4 shows the ratio of the induced density δn to the unperturbed density n_0 at $z = 5$ Å plotted as a function of R for two impurity positions, at $z_0 = 30$ Å and $z_0 = 40$ Å. The potential used is the same as for the solid line in figure 3, with Z_{eff} increased to -0.28 for the deeper impurity to maintain $\delta N(E_{\mathrm{F}}) = 1$. We are restricted to large values of z_0 by the long range of the potential, which is more realistic than using a small value of ρ. The results show the large central peak, followed by rather weak Friedel oscillations.

Translating these results into experiment, the surface corrugation in constant current mode is given by

$$\delta h \approx \frac{\hbar}{2\sqrt{2m_e e\phi_{\mathrm{GaAs}}}} \ln\left(1 + \frac{\delta n}{n_0}\right) \tag{6}$$

where ϕ_{GaAs} is the work-function of GaAs [6]. Our results for the impurity at $z_0 = 30$ Å correspond to a height of 0.7 Å for the central peak, and for the impurity at $z_0 = 40$ Å a height of 0.3 Å. These figures are in the range of observed heights, though on the high side given that 30 Å is the maximum depth of impurity which is observed. The peak is dominated by the bound state, which with our potential parameters has a decay constant of about 0.08 Å^{-1}. STM experiments on $\mathrm{Te_{As}}$-doped GaAs show an exponential decrease in measured peak height with

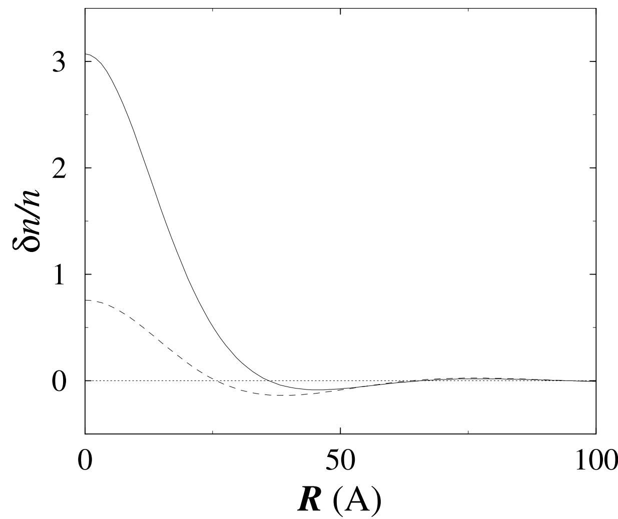

Figure 4. Induced electron density relative to the unperturbed electron density at $z = 5$ Å as a function of R (in Å). Solid line—impurity potential with $Z_{eff} = -0.26$, $\rho = 25$ Å, at $z_0 = 30$ Å; dashed line—with $Z_{eff} = -0.28$, $\rho = 25$ Å, at $z_0 = 40$ Å. The energy has an imaginary part of 2.7 meV.

impurity depth [24], but with a much bigger decay constant of 0.5 Å^{-1}; this seems incompatible with the depth to which the Si impurities are seen.

The Friedel oscillations come from the scattering of the continuum states. Their wavelength with the deeper impurity, for which they are relatively larger, is 71 Å—what we would expect on the basis of the Fermi energy measured from the bottom of the band. Their amplitude varies as $1/R^2$, the behaviour expected with a two-dimensional electron gas [9]. Including the Fermi function for a temperature of 300 K has little effect on the amplitude of the first Friedel oscillation. This lack of sensitivity to temperature broadening has also been found with Friedel oscillations on metal surfaces. It suggests that we have to look elsewhere to explain the reduction (or disappearance) of the Friedel oscillations at room temperature.

A major discrepancy with experiment is the amplitude and position of the Friedel oscillations—experimentally the first minimum has an amplitude of about 1/4 that of the central peak and occurs at $R = 25$ Å, whereas our results for $z_0 = 30$ Å give a tiny minimum at $R = 46$ Å. The experimental results are closer to our results for $z_0 = 40$ Å, even though this is too deep to be imaged! To obtain agreement with experiment we should reduce the bound state contribution, which is in effect what happens with the deeper impurity. Figure 5 shows the separate contributions, from the bound state and from the continuum, to $\delta n/n_0$ for the impurity at $z_0 = 30$ Å, and we see that reducing the bound state contribution to the STM image will enhance the first minimum and pull it in.

This suggests that our assumption that the tunnelling probability is uniform across the states may be incorrect. Even though the exponential decay of the wavefunctions through the barrier is essentially the same [10], we should bear in mind that the tunnelling rate from a localised state can also depend on the rate at which the hole left behind is filled by relaxation processes [24, 25]. If this is the rate-determining step, it will reduce the tunnelling from the bound state. Thermally-activated relaxation would provide an explanation of why the Friedel oscillations are much more apparent at low temperature [24]. However, before we rush to such conclusions it is clear that more work needs to be done on improving our model, with a more

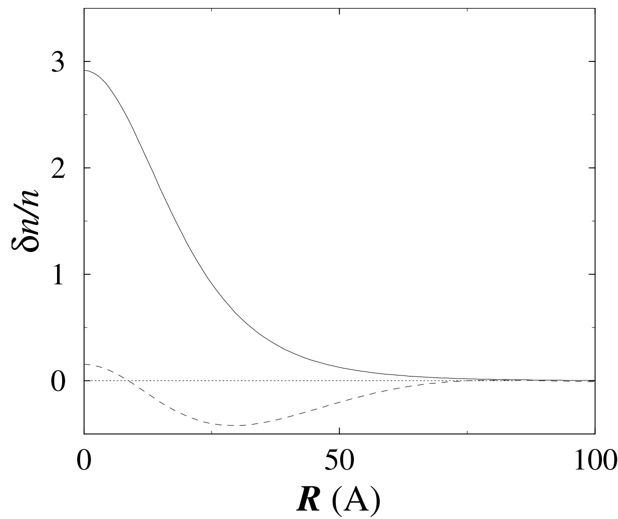

Figure 5. Induced electron density relative to the unperturbed electron density at $z = 5$ Å as a function of R (in Å), with impurity potential with $Z_{\rm eff} = -0.26$, $\rho = 25$ Å, at $z_0 = 30$ Å. Solid line—contribution from bound states; dashed line – contribution from continuum.

realistic (and truly self-consistent) impurity potential, and an accumulation layer which varies across the surface around the STM tip.

The authors are grateful to the British Council and the Dutch Research Council (NWO) for financial support for this collaboration.

References

[1] van der Wielen M C M M, van Roij A J A and van Kempen H 1996 *Phys. Rev. Lett.* **76** 1075
[2] Wenderoth M, Rosentreter M A, Engel K J, Heinrich A J, Schneider M A and Ulbrich R G 1999 *Europhys. Lett.* **45** 579
[3] Zheng J F, Liu X, Newman N, Webster E R, Ogletree D F and Salmeron M 1994 *Phys. Rev. Lett.* **72** 1490
[4] Domke C, Heinrich M, Ebert Ph and Urban K 1998 *J. Vac. Sci. Technol.* B **16** 2825
[5] Pacherová O, Slezák J, Cukr M, and Bartoš I 1999 *Czech. J. Phys.* **49** 1621
[6] Kobayashi K 1996 *Phys. Rev.* B **54** 17 029
[7] Wittneven Chr, Dombrowski R, Morgenstern M and Wiesendanger R 1998 *Phys. Rev. Lett.* **81** 5616
[8] van der Wielen M C M M 1998 *Thesis* University of Nijmegen
[9] Ando T, Fowler A B and Stern F 1982 *Rev. Mod. Phys.* **54** 437
[10] Inglesfield J E and Crampin S 2000 *Phys. Rev.* B **61** 15596
[11] Feenstra R M and Stroscio J A 1987 *J. Vac. Sci. Technol.* B **5** 923
[12] Dombrowski R, Steinebach Chr, Wittneven Chr, Morgenstern M, and Wiesendanger R 1999 *Phys. Rev.* B **59** 8043
[13] Inglesfield J E 1971 *J. Phys. C: Solid State Phys.* **4** L14
[14] Inglesfield J E 1978 *Surface Sci.* **76** 355
[15] Baraff G A and Schlüter M 1984 *Phys. Rev.* B **30** 1853
[16] Landau L D and Lifschitz E M 1965 *Quantum Mechanics* (Oxford: Pergamon Press)
[17] Huant S, Najda S P and Etienne B 1990 *Phys. Rev. Lett.* **65** 1486
[18] Huant S, Mandray A and Etienne B 1995 *Solid State Commun.* **93** 435
[19] Cheng J-P, Li W J, Wang J L, McCombe B D, Holmes S and Schaff W 1995 *Solid State Commun.* **93** 441
[20] Shen J L, Lin T Y, Chen Y F and Chang Y H 1999 *Solid State Commun.* **112** 675
[21] Armistead C J, Najda S P, Stradling R A and Maan J C 1985 *Solid State Commun.* **53** 1109
[22] Huant S, Mandray A, Martinez G, Grynberg M and Etienne B 1992 *Surface Sci.* **263** 565

[23] Pang T and Louie S G 1990 *Phys. Rev. Lett.* **65** 1635
[24] Depuydt A, Van Haesendonck C, Maslova N S, Panov V I, Savinov S V and Arseev P E 1999 *Phys. Rev.* B **60** 2619
[25] de la Broïse X, Delerue C, Lannoo M, Grandidier B and Stiévenard D 2000 *Phys. Rev.* B **61** 2138